BRIEF RESEARCH COMMUNICATION

Right Ventricular to Pulmonary Artery Coupling and Prognosis in Transthyretin Cardiac Amyloidosis

Cardiac amyloidosis (CA) is caused by the extracellular deposition of misfolded proteins, mostly transthyretin (ATTR-CA) or immunoglobulin light-chains (AL-CA), and results in an infiltrative cardiomyopathy with restrictive physiology[1,2]; RV-PA coupling refers to the ability of right ventricular (RV) systolic function to face a given pulmonary afterload and can be noninvasively estimated by calculating the ratio of tricuspid annular plane systolic excursion (TAPSE) to pulmonary artery systolic pressure (PASP) on echocardiography.[3] Reduced values of TAPSE/PASP have been reported as a strong predictor of poor outcomes in different clinical settings.[3-5] In the present study, we aimed to evaluate the prognostic impact of TAPSE/PASP in a large, multicenter cohort of patients with ATTR-CA.

We retrospectively evaluated consecutive patients diagnosed with ATTR-CA from 2005 to 2022 who were enrolled in the International Cardiac Amyloidosis Registry (ICAR). Exclusion criteria are detailed in the supplementary materials. Disease diagnosis was made according to current guidelines.[1]

Tricuspid annular plane systolic excursion was measured on M-mode recordings of the lateral tricuspid annulus, whereas PASP was calculated from the peak velocity of the tricuspid regurgitation (TR) jet according to the Bernoulli equation plus the estimated right atrial pressure, by transthoracic echocardiography. The ratio between TAPSE and PASP was adopted as a noninvasive surrogate of RV-PA coupling.[3-5] A threshold of TAPSE/PASP ≤0.45 mm/mm Hg has been previously reported as prognosticator in patients with CA[6] and has been adopted a priori in the present study. The occurrence of all-cause mortality was the study end point. Statistical methods are detailed in the supplementary materials.

A total of 435 patients were included in the present study (median age, 80 years; 78% male). Most patients had a diagnosis of wild-type ATTR-CA ($n = 352$, 81%), while the remaining 83 cases had hereditary ATTR-CA. The median value of TAPSE/PASP was 0.43 (0.30-0.62) mm/mm Hg and a TAPSE/PASP ≤.45 mm/mm Hg was identified in approximately one-half of the patients ($n = 243$, 55.9%).

Supplemental Tables S1 and S2 show the clinical and echocardiographic features of the overall cohort and stratified by TAPSE/PASP. Patients with TAPSE/PASP ≤0.45 mm/mm Hg were significantly older and had more frequently a diagnosis of wild-type ATTR-CA than their counterparts. They also showed a worse New York Heart Association (NYHA) functional class, a higher prevalence of atrial fibrillation and chronic kidney disease, and higher values of N-terminal pro-B-type natriuretic peptide (NT-proBNP). Patients with TAPSE/PASP ≤0.45 mm/mm Hg had a more advanced cardiomyopathy, as demonstrated by the higher left ventricular (LV) and RV wall thickness, worse LV systolic and diastolic function, and more dilated atria, in comparison to their counterparts. Furthermore, the prevalence of at least moderate mitral regurgitation and TR was significantly higher among patients with TAPSE/PASP ≤ 0.45 mm/mm Hg.

During a median follow-up of 18 months (interquartile range, 10-31 months), 118 patients (27%) died. Individuals with TAPSE/PASP ≤0.45 mm/mm Hg showed a lower survival-rate at 1 and 4 years, as compared with patients with TAPSE/PASP >0.45 mm/mm Hg (82% vs 94% at 1 year and 38% vs 75% at 4 years; both $P < .001$; Figure). The prognostic impact of TAPSE/PASP ≤0.45 mm/mm Hg was confirmed in both subgroups, wild-type and hereditary ATTR-CA (log-rank $P < .001$ and $P = .013$, respectively). On univariable Cox regression analysis, TAPSE/PASP ≤0.45 mm/mm Hg was associated with a remarkably increased risk of death (crude hazard ratio, 2.834; 95% CI, 1.880-4.272, $P < .001$). After extensive multivariable adjustment, RV-PA uncoupling retained an independent association with mortality (adjusted hazard ratio, 1.895; 95% CI, 1.133-3.172; $P = .015$), together with age, NYHA class, LV ejection fraction, and exposure to disease-specific treatment (Table). An alternative multivariable model incorporating NT-proBNP levels, after imputations of the missing data ($n = 81$), confirmed the negative prognostic impact of TAPSE/PASP (data not shown). The addition of RV-PA uncoupling in the multivariable model including its components (TAPSE or PASP) resulted in an incremental predictive value for survival by the likelihood ratio test (change in chi-squared = 3.80, $P = .048$ for TAPSE and change in chi-squared = 10.45, $P < .001$ for PASP).

Our data are in line with the recent study by Tomasoni and colleagues[6] that investigated the clinical implications of RV-PA coupling in a mixed population of 283 patients with CA (53% ATTR-CA and 47% of AL-CA). In their study, a threshold of TAPSE/PASP <.45 mm/mm Hg was significantly associated with an increased risk of the composite of death and heart failure hospitalizations, and this association was confirmed in a subanalysis conducted in the ATTR-CA group, although without multivariable adjustment for other important factors. The present work confirms the negative prognostic value of RV-PA uncoupling in a larger cohort of patients with ATTR-CA when adopting the same threshold of TAPSE/PASP.

Immunoglobulin light chains and ATTR-CA are characterized by crucial differences with respect to epidemiology, pathophysiological substrate of heart failure, clinical course, and prognosis,[2,7] which highlight the importance of individual risk stratification strategies for each CA subtype. This need is further strengthened by the recent availability of specific therapies that have the potential to slow the progression of ATTR-CA and modify the natural course of the disease.[8]

It is worth noting that the use of TAPSE/PASP is limited by the inability to estimate PASP in a proportion of patients because of incomplete TR envelope. Moreover, the threshold adopted in the present study has not been validated versus invasive volume-pressure loop analysis, which still represents the gold standard of RV-PA coupling assessment.

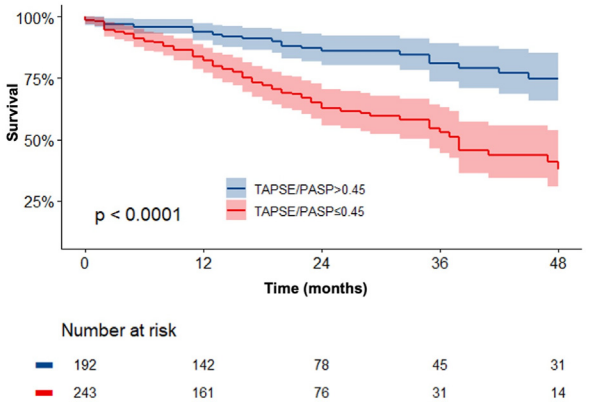

Figure Kaplan-Meier curve for all-cause mortality with 95% confidence limits, stratified by TAPSE/PASP.

Drs. Meucci and Laenens contributed equally to this work and should be considered the same in author order. Drs. Graziani and Ajmone Marsan contributed equally to this work and should be considered the same in author order.

David M. Dudzinski, MD, JD, served as guest editor for this report.

Table Multivariable Cox regression analysis for all-cause mortality

	Adjusted HR (95% CI)	*P* value
Age	1.075 (1.043-1.108)	**<.001**
Hereditary ATTR-CA	0.903 (0.321-2.537)	.846
Chronic kidney disease*	1.149 (0.736-1.794)	.540
Atrial fibrillation	1.341 (0.863-2.084)	.192
NYHA class	1.510 (1.169-1.952)	**.002**
Loop diuretics	1.376 (0.880-2.151)	.162
Disease-specific therapy (time-dependent)	0.564 (0.319-0.998)	**.049**
LV mass index, g/m^2	1.000 (0.995-1.004)	.952
LV ejection fraction, %	0.984 (0.968-1.000)	.057
Moderate or more mitral regurgitation	0.935 (0.588-1.485)	.775
TAPSE/PASP ≤0.45 mm/mm Hg	1.895 (1.133-3.172)	**.015**
Moderate or more TR	1.003 (0.634-1.586)	.991

Statistical significance at the .05 level is shown in bold type.
*Chronic kidney disease is defined by an estimated glomerular filtration rate <60 mL/min/m^2.

FUNDING STATEMENT

This research has been supported by Alnylam (unrestricted research grant to the department of Cardiology of Leiden University Medical Center).

DISCLOSURE STATEMENT

The Department of Cardiology, Heart Lung Center, Leiden University Medical Center, received research grants from Abbott Vascular, Alnylam, Bayer, Bioventrix, Biotronik, Boston Scientific, Edwards Lifescience, GE Healthcare, Medtronic, Medis, Novartis, Pfizer, and Pie Medical. M.C.M. has received travel support from Alnylam. R.L. has received advisory board fees from Sanofi Genzyme, Takeda, and Shire; she has also received travel support from Amicus Therapeutics. P.D. receives Research Grants from Astra Zeneca and received speaker fees from Pfizer, Bayer, and Abbott Vascular. N.A.M. received speaker fees from Abbott Vascular, GE Healthcare, Philips Ultrasound, and Omnor. The remaining authors have nothing to disclose in relation to this paper.

DATA STATEMENT

The data that support the results of this study are available from the corresponding author upon reasonable request.

REVIEW STATEMENT

Given her role as *JASE* Editor-in-Chief, Patricia A. Pellikka, MD, and given her role as *JASE* Associate Editor, Nina Ajmone Marsan, MD, PhD, had no involvement in the peer review of this article and have no access to information regarding its peer review. Full responsibility for the editorial process for this article was delegated to David M. Dudzinski, MD, JD.

SUPPLEMENTARY DATA

Supplementary data related to this article can be found at https://doi.org/10.1016/j.echo.2024.08.013.

Maria Chiara Meucci, MD, Department of Cardiovascular Science, Fondazione Policlinico Universitario A. Gemelli IRCCS, Rome, Italy, Department of Cardiology, Leiden University Medical Center, Leiden, Netherlands
Dorien Laenens, MD, Department of Cardiology, Leiden University Medical Center, Leiden, Netherlands
Rosa Lillo, MD, Antonella Lombardo, MD, Francesco Burzotta, MD, Department of Cardiovascular Science, Fondazione Policlinico Universitario A. Gemelli IRCCS, Rome, Italy, Catholic University of the Sacred Heart, Rome, Italy
Jan Stassen, MD, Department of Cardiovascular Science, Fondazione Policlinico Universitario A. Gemelli IRCCS, Rome, Italy, Department of Cardiology, Jessa Hospital, Hasselt, Belgium
Philippe Debonnaire, MD, PhD, Mathias Claeys, MD, PhD, Department of Cardiology, Sint-Jan Hospital Bruges, Bruges, Belgium
Erwan Donal, MD, PhD, Cardiologie, CHU de RENNES, Université de Rennes, Rennes, France
Steven Droogmans, MD, PhD, Bernard Cosyns, MD, PhD, Vrije Universiteit Brussel (VUB), Universitair Ziekenhuis Brussel (UZ Brussel), Dienst Cardiologie, Centrum voor Hart-en Vaatziekten (CHVZ), Brussels, Belgium
Ruxandra Jurcut, MD, PhD, Department of Cardiology, Expert Center for Rare Genetic Cardiovascular Diseases, Emergency Institute for Cardiovascular Diseases, Bucharest, Romania
Fausto J. Pinto, MD, PhD, Dulce Brito, MD, PhD, Department of Cardiology, Centro Hospitalar Universitário Lisboa Norte, CAML, CCUL@RISE, Faculdade de Medicina, Universidade de Lisboa, Lisboa, Portugal
Idit Yedidya, MD, Department of Cardiology, Rabin Medical Center, Petah Tikva, Tel Aviv, Israel
Caroline Van De Heyning, MD, PhD, Department of Cardiology, University Hospital Antwerp, Antwerp, Belgium, Department of Cardiovascular Sciences, GENCOR Research Group, University of Antwerp, Antwerp, Belgium
Nicole Sturkenboom, MD, Department of Cardiology, University Hospital Antwerp, Antwerp, Belgium
Francesca Graziani, MD, PhD, Department of Cardiovascular Science, Fondazione Policlinico Universitario A. Gemelli IRCCS, Rome, Italy
Nina Ajmone Marsan, MD, PhD, Department of Cardiology, Leiden University Medical Center, Leiden, Netherlands

REFERENCES

1. Garcia-Pavia P, Rapezzi C, Adler Y, et al. Diagnosis and treatment of cardiac amyloidosis. A position statement of the European society of Cardiology working group on myocardial and pericardial diseases. Eur J Heart Fail 2021;23:512-26.
2. Binder C, Duca F, Stelzer PD, et al. Mechanisms of heart failure in transthyretin vs. light chain amyloidosis. Eur Heart J Cardiovasc Imaging 2019;20:512-24.

3. Meucci MC, Malara S, Butcher SC, et al. Evolution and prognostic impact of right ventricular-pulmonary artery coupling after transcatheter aortic valve replacement. JACC Cardiovasc Interv 2023;16:1612-21.
4. Tello K, Wan J, Dalmer A, et al. Validation of the tricuspid annular plane systolic excursion/systolic pulmonary artery pressure ratio for the assessment of right ventricular-arterial coupling in severe pulmonary hypertension. Circ Cardiovasc Imaging 2019;12:e009047.
5. Guazzi M, Dixon D, Labate V, et al. RV contractile function and its coupling to pulmonary circulation in heart failure with preserved ejection fraction: stratification of clinical phenotypes and outcomes. J Am Coll Cardiol Img 2017;10:1211-21.
6. Tomasoni D, Adamo M, Porcari A, et al. Right ventricular to pulmonary artery coupling and outcome in patients with cardiac amyloidosis. Eur Heart J Cardiovasc Imaging 2023;24:1405-14.
7. Rapezzi C, Merlini G, Quarta CC, et al. Systemic cardiac amyloidoses: disease profiles and clinical courses of the 3 main types. Circulation 2009;120:1203-12.
8. Elliott P, Drachman BM, Gottlieb SS, et al. Long-term survival with tafamidis in patients with transthyretin amyloid cardiomyopathy. Circ Heart Fail 2022;15:e008193.

https://doi.org/10.1016/j.echo.2024.08.013

SUPPLEMENTARY MATERIALS

Study population

A total of 731 patients were screened for the current analysis. Patients were excluded from the analysis in case of: 1) incomplete echocardiographic assessment (i.e. missing data for TAPSE or PASP) (n = 20); 2) uninterpretable tricuspid regurgitation TR jet signal to estimate PASP (n = 227); and 3) unavailable clinical follow-up of at least 6 months (n = 61).

Statistical methods

Cumulative survival rates in the study population stratified based on TAPSE/PASP were calculated using the Kaplan-Meier method and compared using the log-rank test. Univariable and multivariable Cox regression analyses were used to investigate the prognostic value of TAPSE/PASP and its components. Multivariable analyses were performed including a maximum of 12 variables, in order to avoid model overfitting. Particularly, these models were built including covariates that were unbalanced between the two groups and/or associated with an increased risk of mortality at univariable analysis ($P < 0.05$ and with the highest Wald test statistics) and with an amount of missing values that did not exceed 5% of the total study population: age, wild-type/hereditary disease, atrial fibrillation, chronic kidney disease, New York Heart Association functional class, use of loop diuretics, disease-specific treatment, LV mass index, LV ejection fraction, moderate or severe mitral regurgitation and moderate or severe TR. Exposure to disease-specific treatment (tafamidis or TTR gene silencers) was included in the models as a binary time-dependent covariate (based on the time of the first initiation of the therapy). The proportional hazards assumption was verified based on Schoenfeld residuals. Significant collinearity was excluded for each multivariable model estimating the variance inflation factor (<0.5). A sensitivity analysis was performed including N-terminal pro-B-type natriuretic peptide (NT-proBNP) levels as covariate and using multiple imputation to account for missing data (n = 81, 19%). Particularly, we generated 30 multiple imputed datasets and the results were combined using Rubin rules. Finally, the incremental prognostic value of TAPSE/PASP over its components (TAPSE and PASP) was assessed by the likelihood ratio chi-square test for nested models.

Supplemental Table 1 Baseline features of the overall cohort and stratified according to TAPSE/PASP

	Total cohort (n = 435)	TAPSE/PASP >0.45 mm/mm Hg (n = 192)	TAPSE/PASP ≤0.45 mm/mm Hg (n = 243)	*P*-value
Clinical features				
Age (years)	80 (73-85)	77 (67-82)	82 (75-86)	**<.001**
Female gender (n, %)	94 (22)	42 (22)	52 (21)	.95
Wild-type/hereditary (n, %)	352 (81)/83 (19)	133 (69)/59 (31)	219 (90)/24 (10)	**<.001**
BMI (kg/m^2)	24.1 ± 4.0	24.4 ± 4.2	23.9 ± 3.8	.218
Diabetes mellitus (n, %)	64 (15)	22 (11)	42 (17)	.102
Arterial hypertension (n, %)	258 (59)	107 (56)	151 (62)	.283
CAD (n, %)	102 (23)	40 (21)	62 (26)	.296
CKD* (n, %)	197 (45)	60 (31)	137 (56)	**<.001**
AF (n, %)	222 (51)	69 (36)	153 (63)	**<.001**
PM/ICD (n, %)	81 (19)	29 (15)	52 (21)	.090
NYHA class (n, %)				**<.001**
I	96 (22)	67 (35)	30 (12)	
II	209 (48)	92 (48)	114 (47)	
III/IV	130 (30)	33 (17)	99 (41)	
SBP (mm Hg)	127 ± 22	129 ± 22	126 ± 21	.257
NT-proBNP† (pg/ml)	2438 (848-4901)	1072 (351-2258)	3854 (2281-8755)	**<.001**
NAC stage† (%)	54/27/19	77/18/5	33/34/32	**<.001**
Medications				
Beta-blockers (n, %)	230 (53)	98 (51)	132 (54)	.602
ACEi/ARB (n, %)	203 (47)	88 (46)	115 (47)	.869
Loop diuretics (n, %)	231 (53)	70 (36)	161 (66)	**<.001**
MRA (n, %)	148 (34)	37 (19)	111 (56)	**<.001**
Oral anticoagulants (n, %)	197 (45)	61 (32)	136 (57)	**<.001**
Tafamidis/TTR gene silencers at baseline (n, %)	58 (13)/8 (2)	20 (10)/5 (3)	38 (16)/3 (1)	.176

Statistically significance at the 0.05 level is shown in bold type.

ACEi/ARB, Angiotensin-converting enzyme inhibitors or angiotensin receptor; *AF*, atrial fibrillation; *BMI*, body mass index; *CAD*, coronary artery disease; *CKD*, chronic kidney disease; *MRA*, mineralocorticoid receptor antagonist; *NYHA*, New York Heart Association; *NT-proBNP*, N-terminal pro-B-type natriuretic peptide; *PM/ICD*, pacemaker/implanted cardioverter defibrillator; *SBP*, systolic blood pressure; *TTR*, transthyretin.

*CKD defined by an estimated glomerular filtration rate <60 ml/min/m^2.

†NT-proBNP levels and NAC staging were available in 354 (81% of the patients).

Supplemental Table 2 Echocardiographic data of the overall cohort and stratified according to TAPSE/PASP

	Total cohort (n = 435)	TAPSE/PASP >0.45 mm/mm Hg (n = 192)	TAPSE/PASP ≤0.45 mm/mm Hg (n = 243)	*P*-value
IVS thickness (mm)	16.8 ± 3.5	16.0 ± 3.1	17.5 ± 3.6	**<.001**
PW thickness (mm)	15.0 ± 3.7	13.9 ± 3.0	15.8 ± 4.0	**.004**
LVEDD (mm)	44.1 ± 6.8	44.7 ± 6.7	44.3 ± 6.9	.111
LVESD (mm)	31.3 ± 7.3	30.1 ± 7.1	32.2 ± 7.4	.407
LVMi (g/m^2)	166 ± 53	151 ± 47	178 ± 55	**<.001**
LVEF (%)	50.7 ± 12.4	55.5 ± 10.5	47.0 ± 12.5	**<.001**
LVGLS* (%)	12.0 ± 4.1	14.1 ± 4.0	10.2 ± 3.3	**<.001**
LAVi (ml/m^2)	48.9 (40.0-60)	44.0 (36.0-55.5)	52.9 (45.0-64.7)	**<.001**
E/A ratio	1.6 (1.1-2.6)	1.2 (0.9-1.9)	2.1 (1.4-2.9)	**<.001**
E/e' ratio	17.0 (12.2-23.0)	15.0 (10.7-19.4)	19.0 (15.0-25.7)	**<.001**
RA area (cm^2)	20.0 (17.0-25.4)	18.7 (15.5-21.9)	22.5 (18.6-27.0)	**<.001**
RVWT (mm)	7.0 (6.0-8.5)	6.0 (5.1-7.3)	8.0 (6.0-9.0)	**<.001**
TAPSE (mm)	17.3 ± 5.1	20.8 ± 4.2	14.5 ± 3.9	**<.001**
RVFAC (%)	36.6 (27.3-44.6)	41.7 (35.2-47.9)	32.4 (23.2-41.2)	**<.001**
PASP (mm Hg)	41 ± 13	31 ± 8	48 ± 11	**<.001**
TAPSE/PASP (mm/mm Hg)	0.43 (0.30-0.62)	0.65 (0.53-0.83)	0.31 (0.25-0.38)	**<.001**
≥ moderate MR (n, %)	126 (29)	37 (19)	89 (37)	**<.001**
≥ moderate TR (n, %)	142 (33)	26 (14)	116 (48)	**<.001**

Statistically significance at the 0.05 level is shown in bold type.

IVS, Interventricular septum; *LAVi*, left atrium volume index; *LV*, left ventricular; *LVEDD*, LV end-diastolic diameter; *LVESD*, LV end-systolic diameter; *LVEF*, LV ejection fraction; *LVMi*, left ventricular mass index; *LVGLS*, LV global longitudinal strain; *PW*, posterior wall; *MR*, mitral regurgitation; *PASP*, pulmonary artery systolic pressure; *RA*, right atrium; *RVWT*, right ventricular wall thickness; *RVFAC*, right ventricular fractional area change; *TAPSE*, tricuspid annular plane systolic excursion; *TR*, tricuspid regurgitation.

*LVGLS was available in 350 patients, due to the availability of archived images for analysis.

.